Volume 1 | Number 1 | Jan 2013 | Pages 1–100

Nanoscale

www.rsc.org/nanoscale

ROYAL SOCIETY OF CHEMISTRY

ROYAL SOCIETY OF CHEMISTRY

www.rsc.org/nanoscale

Nanoscale

ARTICLE

Tuning of photoluminescence and up-conversion photoluminescence properties of single-walled carbon nanotubes by chemical functionalization

Yutaka Maeda,[a],* Shun Minami,[a] Yuya Takehana,[a] Jing-Shuang Dang,[b] Shun Aota,[c] Kazunari Matsuda,[c] Yuhei Miyauchi,[c],* Michio Yamada,[a] Mitsuaki Suzuki,[a] Rui-Sheng Zhao,[d] Xiang Zhao,[d] Shigeru Nagase[b],*

Single-walled carbon nanotubes (SWNTs) were subjected to alkylation using alkyl bromide and alkyl dibromide, and the photoluminescence (PL) properties of the resulting alkylated SWNTs were characterized. Two new PL peaks were observed along with the intrinsic PL peak at 976 nm when alkyl bromide was used (SWNTs-Bu: ~1095 and 1230 nm, SWNTs-Bn: 1104 and 1197 nm). In contrast, the use of α,α'-dibromo-o-xylene as a alkyl dibromide primarily resulted in only one new PL peak, which was observed at 1231 nm. The results revealed that the Stokes shift of the new peaks was strongly influenced by the addition patterns of the substituents. In addition, the time-resolved PL decay profiles of the alkylated SWNTs revealed that the PL peaks possessing larger Stokes shift had longer exciton lifetimes. The up-conversion PL (UCPL) intensity of the alkylated SWNTs at excitation wavelengths of 1100 and 1250 nm was estimated to be ~2.38 and ~2.35 times higher than that of the as-dispersed SWNTs, respectively.

1. Introduction

Single-walled carbon nanotubes (SWNTs) have excellent mechanical and electrical properties, which make them suitable for various applications.[1,2] The photoluminescence (PL) properties of semiconducting SWNTs in the near-infrared (NIR) region were studied for the first time in 2002.[2,3] PL spectroscopy is a very powerful tool for the investigation of PL properties of semiconducting SWNTs as it can separately generate the E_{11} PL peaks of individual SWNTs by the excitation of the E_{22} transitions. Recently, NIR light has received significant attention in bio-imaging applications owing to the high transparency of biological tissues to it.[5-8] To improve the performance of SWNTs as biological imaging materials, chirality-separated semiconducting SWNTs have been investigated, and have exhibited superior performance than their non-separated counterparts.[9] Sidewall functionalization of SWNTs results in a new, bright, and red-shifted PL peak (E_{11}^* PL peak).[10-15] Sidewall functionalization is an effective method for controlling the PL characteristics of SWNTs for practical applications as the

introduction of new functionalities onto the SWNTs improves their dispersibility.[16] In addition, owing to their large Stokes shifts, functionalized SWNTs can be excited by the E_{11} energy at which the transparency of biological tissues is higher than that at the E_{22} energy. Large Stokes shift allows easy elimination of Rayleigh scattering. Wang et al. reported that the peak energy of the new PL peak in SWNTs can be tuned to fall within the range 1110–1148 nm owing to the effect of 4-substituted phenyl groups on SWNTs.[13] Recently, we reported that the dialkylation of SWNTs using butyllithium and butyl bromide and their subsequent thermal treatment results in a new strong PL peak in the NIR region.[15,17] The dibutylated SWNTs obtained after the thermal treatment exhibited a larger Stokes shift at ~1210 nm than those exhibited by the oxidized, arylated, and alkylcarboxylated SWNTs (See Table S1). In addition, the theoretical studies predicted that the band structure of the functionalized SWNTs was influenced by the local structures of the addition sites and the distance of the addition site carbons of the substituents.[19,20] In this study, we demonstrate reductive alkylation of SWNTs using alkyl bromides (^{n}butyl bromide (^{n}BuBr), isobutyl bromide (^{i}BuBr), ^{sec}butyl bromide (^{sec}BuBr), benzyl bromide (BnBr)) and alkyl dibromide (α,α'-dibromo-o-xylene) and characterize their PL and UCPL properties.

2. Experimental Section

2.1 Typical procedure of reductive alkylation.

Naphthalene (300 mg, 2.34 mmol) and sodium (150 mg, 6.52 mmol) in a 200 mL heat-dried three-necked round-bottom flask were placed under argon. Anhydrous tetrahydrofuran (100 mL) was then added to

[a.] Department of Chemistry, Tokyo Gakugei University, Koganei, Tokyo 184-8501, Japan. E-mail: ymaeda@u-gakugei.ac.jp
[b.] Fukui Institute for Fundamental Chemistry, Kyoto University, Sakyou-ku, Kyoto 606-8103, Japan.
[c.] Institute of Advanced Energy, Kyoto University, Uji, Kyoto 611-0011, Japan.
[d.] Institute for Chemical Physics & Department of Chemistry, State Key Laboratory of Electrical Insulation and 5Power Equipment, Xi'an Jiaotong University, Xi'an 710049, China

the flask and the contents were stirred for 30 min. A portion (10.0 mg) of SWNTs in a 200 mL heat-dried three-necked round-bottom flask was placed under argon. The sodium naphthalenide solution was added to the SWNTs, which were then sonicated for 30 min, and butyl bromide (2.84 mmol) was subsequently added to the mixture. The mixture was sonicated for 1 h and then quenched by the addition of 30 mL of dry ethanol. Afterwards, the reaction mixture was washed with water and diluted in 10% HCl aq. and subsequently washed with $NaHCO_3$ aq. until a neutral pH value was obtained. The resulting suspended black solid was collected by means of filtration using a membrane filter (PTFE, 1.0 μm) and washed with tetrahydrofuran, methanol, and dichloromethane via the dispersion-filtration process. The solid was then dried under vacuum at 50 °C.

2.2 Thermal treatment of alkylated SWNTs.

The SWNTs-(^{n}Bu) were thermally treated at a heating rate of 10 °C/min and a nitrogen flow rate of 50 mL/min by using a thermogravimetric analyzer (TG-50A; Shimadzu Corp.). After reaching 200 ℃, the SWNTs-(^{n}Bu) was continuously hated for 6 h at 200 ℃, and then heating furnace was cooled, by using a cooling blower (BLW-50 cooling blower; Shimadzu Corp.).

2.3 Preparation of SWNTs dispersion using SDBS in D_2O.

A portion of SWNTs or functionalized SWNTs (SWNTs-R) was added to 4 mL of D_2O containing 1 wt% sodium dodecylbenzenesulfonate (SDBS) and sonicated for 1.5 h in a bath-type sonicator (Branson ultrasonic cleaner 2510 J-MT). This suspension was then centrifuged for 1 h at 140,000 g. The absorption intensity at ~775 nm was adjusted, by adding an adequate dose of D_2O solution containing 1 wt% of SDBS to the supernatant solution. After 10 min of sonication, the resulting suspension was centrifuged for 1 h at 140,000 g. The absorption intensities of the SWNTs and functionalized SWNTs for PL measurements are listed in Table S2.

2.4 Measurements of time resolved PL and UCPL.

A supercontinuum white-light source (Fianium, SC450) was used as an excitation light source for measurements of both time-resolved photoluminescence decay profiles and up-conversion photoluminescence spectra. The excitation light wavelengths for each measurement were selected using multiple optical filters. The time-resolved photoluminescence decay profiles were recorded using a time correlated single-photon counting technique under pulsed excitation (40 MHz, ~10 ps pulse duration at a photon wavelength of 830 nm) with a liquid helium-cooled superconducting single photon detecting system (SCONTEL) operated at ~2K. The photoluminescence from each peak feature was separated using optical filters with a band-pass of 10 nm. To obtain the effective PL lifetimes, we fitted the data using the convolution of the instrumental response function (IRF) with Kohlrausch function (for free excitons) and double exponential function (for localized excitons) to obtain the original photoluminescence decay profiles of free and localized excitons. Up-conversion PL spectroscopy was performed using a Si-based charge coupled device (CCD) cooled with liquid nitrogen (Princeton Instruments, SPEC-10). The reflection-mode confocal microscopic optical configurations with a 0.42 NA, ×50 objective were used for the optical measurements. All measurements were performed on samples placed in a quartz cell at room temperature.

2.5 Theoretical studies.

A hydrogen-terminated (6,6)-SWNT structure containing 21 carbon layers ($C_{252}H_{24}$) was employed to study the spin density distribution of Bu-(6,6)-SWNTs radical in which the Bu group is binding on the center carbon layer. Structural optimization was performed using Gaussian 09 within the DFT framework using the B3LYP functional in conjunction with the 6-31G(d) basis set.[21-24]

3. RESULTS AND DISCUSSION

The alkylated SWNTs (SWNTs-R) were synthesized using sodium naphthalenide and alkyl bromide (RBr; R = ^{n}Bu, ^{i}Bu, and ^{s}Bu) (Scheme 1).[25,26] The degree of functionalization was estimated from the intensity ratio of the D/G bands in the Raman spectra of SWNTs-Bu (Fig. 1a, b). Successful sidewall functionalization was confirmed by an increase in the D/G ratio with a decrease in the intensity of the radial breathing mode (RBM) peaks after the reductive reaction.[27]

During the reductive alkylation, it was difficult to measure the in situ absorption and PL characteristics of the SWNTs owing to their low dispersibility under the reaction conditions employed. The SWNTs and functionalized SWNTs were therefore dispersed in a D_2O solution containing 1 wt% of SDBS and the resulting dispersions were then centrifuged at 140,000 g. In order to compare the characteristic absorption and PL peak intensities before and after functionalization, SWNT dispersions having absorption intensities of 0.0735 ± 0.0085 and a local minimum at ~775 nm were prepared (see Table S2). This local minimum was selected because the absorption intensity at ~775 nm changes only slightly as compared to the intensity of the E_{11} characteristic peak in the photochemical reactions of the SWNTs with aliphatic amines.[28] The weak characteristic E_{11} and E_{22} absorption peaks of SWNTs-Bu were consistent with the Raman spectroscopy results (Fig. 1a-c).

Two new PL peaks were observed at ~1100 (E_{11}^*) and ~1230 nm (E_{11}^{**}) in the PL spectra of SWNTs-Bu (Fig. 1d). According to previous reports, each of the oxidized (SWNTs-O: 1120 nm),[10] arylated (SWNTs-Ph: 1119 nm),[13] alkylcarboxylated (SWNTs-$(CH_2)_5COOH$: 1091 nm),[14] and dialkylated SWNTs after thermal treatment at 300 ℃ (^{n}Bu-SWNTs-^{n}Bu (300 °C): 1213 nm) typically give rise to mainly one new peak.[15]

In this work, we focused our attention on the intermediates of Bu-SWNTs-Bu and SWNTs-Bu, which have the same substituent groups. The difference in the distance of the addition site carbon atoms of the substituents may therefore account for the difference in the PL properties of Bu-SWNTs-Bu and SWNTs-Bu. As shown in Schemes 1 and 2, the Bu-SWNT and SWNT radicals were plausible intermediates for Bu-SWNTs-Bu and SWNTs-Bu, respectively. The theoretical calculations using the density functional theory revealed that the spin density of the Bu-SWNT radical was localized at the neighbouring carbon atoms of the addition site (Fig. 2). Therefore, the second butyl group could be introduced at the carbon atoms in the neighbourhood of the addition site carbon when butyllithium and butyl bromide were used. On the other hand, owing to the delocalization of the spin density of the SWNT radical, the butyl radicals could be introduced everywhere during the initial stage of the reaction between the SWNT and butyl radicals. Thus, we can

state that the addition of butyl radicals probably took place at the carbon atoms distant from the other addition site carbon atoms during the initial stage when sodium naphthalenide and butyl bromide were used.
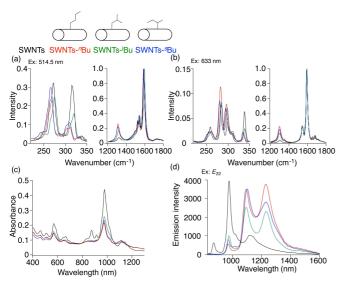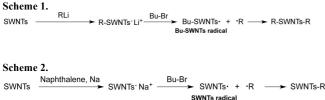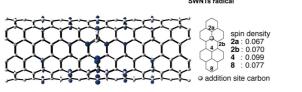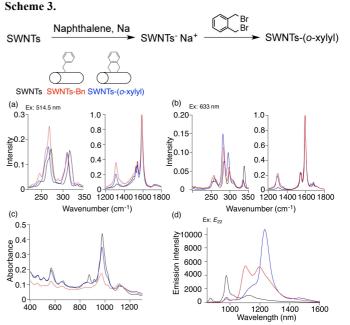

Fig. 1. (a,b) Raman, (c) absorption, and (d) PL spectra of SWNTs and SWNTs-Bu.

Scheme 1.

Scheme 2.

Fig. 2. Spin density of ^{n}Bu-(6,6)SWNT radical. The hydrogen atoms at edge are omitted for clarity.

The effect of the addition patterns of the substituents on the PL properties of alkylated SWNTs was further investigated through the reductive alkylation of SWNTs with alkyl dibromide. In this study, α,α'-dibromo-o-xylene was selected because this dihalide is used in the synthesis of 1,2-cycloaddition products of C_{60}.[29,30] Interestingly, SWNTs-(o-xylyl), prepared with α,α'-dibromo-o-xylene gave rise to only one new PL peak at 1231 nm. In contrast, the benzylated SWNTs (SWNTs-Bn) prepared with benzyl bromide, yielded two new peaks at 1104 and 1197 nm. The results indicate that the positions of the PL peaks obtained after functionalization were strongly influenced by the distance between the addition site carbon atoms of the substituents (Fig. 3). Counter plots of the fluorescence intensity versus excitation and emission wavelength of the functionalized SWNTs (Fig. 4) revealed strong emission at E_{11} excitation after the functionalization. As previously mentioned, the

excitation of functionalized SWNTs by a high-efficiency NIR light is well-suited for applications such as biological imaging.

Scheme 3.

Fig. 3. (a,b) Raman, (c) absorption, and (d) PL spectra of SWNTs and functionalized SWNTs.

The UCPL properties of SWNTs, which possess properties such as high transparency and low phototoxicity in biological tissues, have received a great deal of attention. Akizuki et al. have recently reported that relatively efficient UCPL can be observed in oxidized and arylated SWNTs.[31] It was reported that the UCPL intensities of oxidized SWNTs and arylated SWNTs at an excitation wavelength of 1148 nm (1.08 eV) are approximately 3 times higher than that of unfunctionalized SWNTs, respectively. This suggests that since the excitation energy of UCPL closely matched the PL peak energies of the oxidized and arylated SWNTs, the localized states generated by the chemical functionalization acted as intermediate states for excitation in the up-conversion processes.[1] The UCPL measurements of SWNTs-^{n}Bu(Δ) were conducted to elucidate the relationship between the UCPL intensities and the PL peak energies (E_{11}^* and E_{11}^{**}).
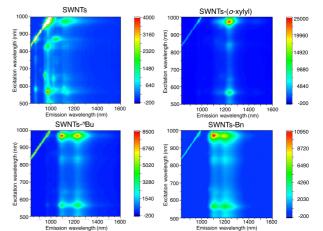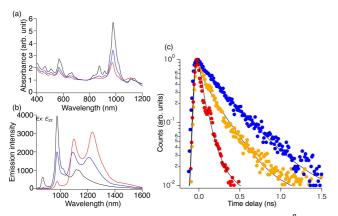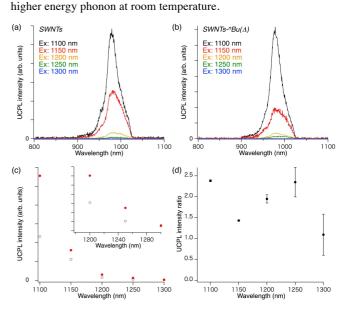

Fig. 4. Counter plots of fluorescence intensity versus excitaion and emission wavelength of SWNTs and funciotnalized SWNTs.

Fig. 5. (a) Absorption spectra of SWNTs (black), SWNTs-^{n}Bu (red), and SWNTs-^{n}Bu(Δ) (blue) normalized at 780 nm. (b) PL spectra of SWNTs (black), SWNTs-^{n}Bu (red), and SWNTs-^{n}Bu(Δ) (blue). (c) Time-resolved PL decay profiles of SWNTs-^{n}Bu(Δ) at an excitation wavelength of 830 nm. The red, yellow, and blue circles indicate the PL decay at 980, 1100, and 1200 nm, respectively.

In a recent study, the luminescence quantum yield of localized excitons in oxidized SWNTs was found to be at least one order larger ($\sim$18%) than that of free excitons (typically $\sim$1%).[12] The high quantum yield of the localized excitons was estimated from the PL lifetime of the free and localized excitons in the oxidized SWNTs, which is approximately six times longer than that of the intrinsic excitons. Here, the measurement of PL lifetimes of SWNTs-^{n}Bu was conducted using the time-correlated single photon counting method to compare the exciton lifetimes at E_{11}, E_{11}^*, and E_{11}^{**}. SWNTs-^{n}Bu, which were thermally treated at 200 °C for 6 h (SWNTs-^{n}Bu(Δ)) for partial removal of substituents and gave rise to the E_{11}, E_{11}^*, and E_{11}^{**} PL peaks, were prepared for the comparison of these exciton lifetimes (Fig. 5). The time-resolved PL decay profiles of SWNTs-^{n}Bu(Δ) at room temperature are shown in Fig. 5c, and the exciton lifetimes at 980, 1100, and 1200 nm were estimated to be $\sim$23, $\sim$65, and $\sim$118 ps, respectively. It is noteworthy that the PL peaks possessing larger Stokes shift had longer exciton lifetimes. This is attributable to longer PL lifetimes resulting in high PL quantum yield. Moreover, larger Stokes shift allows easy elimination of auto-fluorescence in bio-imaging applications.

Fig. 6a,b shows the UCPL spectra of the as-dispersed SWNTs and SWNTs-^{n}Bu(Δ), respectively. The UCPL intensities of both the samples varied depending on the excitation wavelengths. Fig. 6c shows the integrated UCPL intensities as a function of excitation wavelengths. For all the excitation wavelengths, the UCPL intensities of SWNTs-^{n}Bu(Δ) were stronger than that of the as-dispersed SWNTs. Fig. 6d plots the ratio of the UCPL intensities of SWNTs-^{n}Bu(Δ) to those of the as-dispersed SWNTs at each excitation wavelength. It can clearly be observed that the UCPL intensities of SWNTs-^{n}Bu(Δ) were high at the wavelengths corresponding to E_{11}^* ($\sim$1,13 eV (1100 nm)) and E_{11}^{**} ($\sim$1.0 eV (1250 nm)) as compared to those of the as-dispersed SWNTs. Since the UCPL of SWNTs has been attributed to the efficient phonon-assisted energy up-conversion processes from the localized to free exciton states, the increase in peak intensity in the UCPL spectra of SWNTs-^{n}Bu(Δ) is attributable to an increase in the number of initially created localized excitons with energies of E_{11}^* and E_{11}^{**} at the functionalized sites. Furthermore, the lower UCPL intensity for larger energy gain for both the as-dispersed SWNTs and SWNTs-

^{n}Bu(Δ) is attributable to the decrease in the number of phonons for higher energy phonon at room temperature.

Fig. 6 (a), (b) Excitation wavelength dependence of the PL spectra of as-dispersed SWNTs and SWNTs-^{n}Bu(Δ). (c) Integrated UCPL intensity vs. excitation wavelength for as-dispersed SWNTs (○) and SWNTs-^{n}Bu(Δ) (●). Inset: Expanded views in 1180 − 1300 nm. (d) Ratio of the spectral integrated UCPL intensity of as-dispersed SWNTs and SWNTs-^{n}Bu(Δ) (I_doped/I_as-dispersed) as a function of excitation wavelength.

4. Conclusions

In conclusion, we have studied the PL and UCPL properties of alkylated SWNTs prepared using alkyl bromide and alkyl dibromide. Two new PL peaks were observed when alkyl bromide was used (SWNTs-Bu: $\sim$1095 and 1230 nm. SWNTs-Bn: 1104 and 1197 nm). In contrast, the use of α,α'-dibromo-o-xylene primarily resulted in only one new PL peak. The results indicate that as two-step reductive alkylation, the cycloaddition reaction of SWNTs using alkyl dibromide is effective to generate new and strong PL peak with large Stokes shift. In addition, the time-resolved PL decay profiles of the alkylated SWNTs revealed that the PL peaks possessing larger Stokes shift had longer exciton lifetimes. The UCPL efficiency of the alkylated SWNTs at the excitation wavelengths of 1100 and 1250 nm was estimated to be $\sim$2.38 and $\sim$2.35 times higher than that of the as-dispersed SWNTs, respectively. Controlling the distance of the addition site carbons is a simple method for controlling the Stokes shift, emission efficiency, lifetime, and up-conversion efficiency of NIR PL. This method is highly desirable owing to its applicability in various NIR PL applications.

Acknowledgements

References

1 S. Iijima and T. Ichihashi, *Nature*, 1993, **363**, 603-605.
2 D. S. Bethune, C. H. Kiang, M. S. De Vries, G. Gorman, R. Savoy, J. Vazquez and R. Beyers, *Nature*, 1993, **363**, 605-607.
3 S. M. Bachilo, M. S. Strano, C. Kittrell, R. H. Hauge, R. E. Smalley and R. B. Weisman, *Science*, 2002, **298**, 2361-2366.
4 M. J. O'Connell, S. M. Bachilo, C. B. Huffman, V. C. Moore, M. S. Strano, E. H. Haroz, K. L. Railon, P. J. Boul, W. H. Noon, C. Kittrell, J. Ma, R. H. Hauge, R. B. Weisman and R. E. Smalley, *Science*, 2002, **297**, 593-596.
5 R. Weisskeder, *Nature Biotechnology*, 2001, **19**, 316-317.
6 P. Cherukuri, S. M. Bachilo, S. H. Litovsky and R. B. Weisman, *J. Am. Chem. Soc.*, 2004, **126**, 15638-15639.
7 P. Cherukuri, C. J. Gannon, T. K. Leeuw, H. K. Schmidt, R. E. Smalley, S. A. Curley and R. B. Weisman, *Proc. Nat. Acad. Sci. U.S.A.*, 2006, **103**, 18882-18886.
8 K. Welsher, S. P. Sherlock and H. Dai, *Proc. Nat. Acad. Sci. U.S.A.*, 2011, **108**, 8943-8948.
9 S. Diao, G. Hong, J. T. Robinson, L. Jiao, A. L. Antaris, J. Z. Wu, C. L. Choi and H. Dai, *J. Am. Chem. Soc.*, 2012, **134**, 16971-16974.
10 S. Ghosh, S. M. Bachilo, R. A. Simonette, K. M. Beckingham and R. B. Weisman, *Science*, 2010, **330**, 1656-1659.
11 Y. Maeda, J. Higo, Y. Amagai, J. Matsui, K. Ohkubo, Y. Yoshigoe, M. Hashimoto, K. Eguchi, M. Yamada, T. Hasegawa, Y. Sato, J. Zhou, J. Lu, T. Miyashita, S. Fukuzumi, T. Murakami, K. Tohji, S. Nagase and T. Akasaka, *J. Am. Chem. Soc.*, 2013, **135**, 6356-6362.
12 Y. Miyauchi, M. Iwamura, S. Mouri, T. Kawazoe, M. Ohtsu and K. Matsuda, *Nat. Photon.*, 2013, **7**, 715-719.
13 Y. Piao, B. Meany, L. R. Powell, N. Valley, H. Kwon, G. C. Schatz and Y. Wang, *Nat. Chem.*, 2013, **5**, 840-845
14 Y. Zhang, N. Valley, A. H. Brozena, Y. Piao, X. Song, G. C. Schatz and Y. Wang, *J. Phys. Chem. Lett.*, 2013, **4**, 826-830.
15 Y. Maeda, Y. Takehana, M. Yamada, M. Suzuki and T. Murakami, *Chem. Commun.*, 2015, **51**, 13462-13465.
16 J. Chen, M. A. Hamon, H. Hu, Y. Chen, A. M. Rao, P. C. Eklund and R. C. Haddon, *Science*, 1998, **282**, 95-98.
17 Y. Maeda, T. Kato, T. Hasegawa, M. Kako, T. Akasaka, J. Lu and S. Nagase, *Organic Lett.*, 2010, **12**, 996-999.
18 Y. Maeda, K. Saito, N. Akamatsu, Y. Chiba, S. Ohno, Y. Okui, M. Yamada, T. Hasegawa, M. Kako and T. Akasaka, *J. Am. Chem. Soc.*, 2012, **134**, 18101-18108.
19 S. Kilina, J. Ramirez and S. Tretiak, *Nano Lett.*, 2012, **12**, 2306-2312.
20 X. Ma, L. Adamska, H. Yamaguchi, S. E. Yalcin, S. Tretiak, S. K. Doorn and H. Htoon, *ACS Nano*, 2014, **8**, 10782-10789.
21 A. D. Becke, *J. Chem. Phys.* 1993, **98**, 5648-5652.
22 C. Lee, W. Yang and R. G. Parr, *Phys. Rev. B*, 1998, **37**, 785-789.
23 M. N. Berberan-Santos, E. N. Bodunov and B. Valeur, *Chem. Phys.*, 2005, **315**, 171-182.
24 Gaussian 09, Revision D.01, M. J. Frisch, G. W. Trucks, H. B. Schlegel, G. E. Scuseria, M. A. Robb, J. R. Cheeseman, G. Scalmani, V. Barone, B. Mennucci, G. A. Petersson, H. Nakatsuji, M. Caricato, X. Li, H. P. Hratchian, A. F. Izmaylov, J. Bloino, G. Zheng, J. L. Sonnenberg, M. Hada, M. Ehara, K. Toyota, R. Fukuda, J. Hasegawa, M. Ishida, T. Nakajima, Y. Honda, O. Kitao, H. Nakai, T. Vreven, J. A. Montgomery, Jr., J. E. Peralta, F. Ogliaro, M. Bearpark, J. J. Heyd, E. Brothers, K. N. Kudin, V. N. Staroverov, R. Kobayashi, J. Normand, K. Raghavachari, A. Rendell, J. C. Burant, S. S. Iyengar, J. Tomasi, M. Cossi, N. Rega, J. M.

Millam, M. Klene, J. E. Knox, J. B. Cross, V. Bakken, C. Adamo, J. Jaramillo, R. Gomperts, R. E. Stratmann, O. Yazyev, A. J. Austin, R. Cammi, C. Pomelli, J. W. Ochterski, R. L. Martin, K. Morokuma, V. G. Zakrzewski, G. A. Voth, P. Salvador, J. J. Dannenberg, S. Dapprich, A. D. Daniels, Ö. Farkas, J. B. Foresman, J. V. Ortiz, J. Cioslowski, and D. J. Fox, Gaussian, Inc., Wallingford CT, 2009.
25 F. Liang, A. K. Sadana, A. Peera, J. Chattopadhyay, Z. Gu, R. H. Hauge and W. E. Billups, *Nano Lett.*, 2004, **4**, 1257-1260.
26 J.-Y. Mevellec, C. Bergeret, J. Cousseau, J.-P. Buisson, C. P. Ewels and S. Lefrant, *J. Am. Chem. Soc.*, 2011, **133**, 16938-16946.
27 H. Hu, B. Zhao, M. A. Hamon, K. Kamaras, M. E. Itkis and R. C. Haddon, *J. Am. Chem. Soc.*, 2003, **125**, 14893-14900.
28 Y. Maeda, Y. Hasuike, K. Ohkubo, A. Tashiro, S. Kaneko, M. Kikuta, M. Yamada, T. Hasegawa, T. Akasaka, J. Zhou, J. Lu, S. Nagase and S. Fukuzumi, *ChemPhysChem*, 2014, **15**, 1821-1826.
29 R. Subramanian, K. M. Kadish, M. N. Vijayashree, X. Gao, M. T. Jones, M. D. Miller, K. L. Krause, T. Suenobu and S. Fukuzumi, *J. Phys. Chem*, 1996, **100**, 16327-16335.
30 E. Allard, L. Riviere, J. Delaunay, D. Dubois and J. Cousseau, *Tetrahedron Lett.*, 1999, **40**, 7223-7226.
31 N. Akizuki, S. Aota, S. Mouri, K. Matsuda and Y. Miyauchi, *Nat. Commun.*, 2015, **16**, 8920.
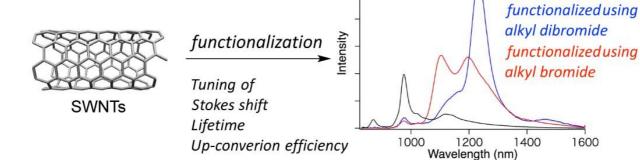
Controlling the NIR-PL properties of SWNTs by chemical functionalization